ISSN 0027-1314, Moscow University Chemistry Bulletin, 2011, Vol. 66, No. 5, pp. 290–298. © Allerton Press, Inc., 2011.
Original Russian Text © A.V. Maryashkin, Yu.D. Ivakin, M.N. Danchevskaya, G.P. Murav'eva, M.N. Kirikova, 2011, published in Vestnik Moskovskogo Universiteta. Khimiya, 2011, No. 5, pp. 352–362.

Synthesis of Corundum Doped with Cerium in Supercritical Water Fluid

A. V. Maryashkin, Yu. D. Ivakin, M. N. Danchevskaya, G. P. Murav'eva, and M. N. Kirikova

Division of Physical Chemistry, Department of Chemistry, Moscow State University, Moscow, Russia

e-mail: Ivakin@kge.msu.ru

Received April 20, 2011

Abstract—The properties of fine crystalline corundum doped with cerium (α-Al_2O_3 : Ce^{3+}) during synthesis in a supercritical fluid have been studied. The synthesis of corundum has been carried out by the thermal treatment of hydrargillite, $Al(OH)_3$, at $T = 415$°C and $P_{H_2O} = 21–31$ MPa in reaction media that contained from 0.001 to 0.25 wt % of cerium. Cerium ions are incorporated into the boehmite lattice during the transformation of hydrargillite into boehmite, which forms fine monocrystals of the doped corundum with a size from 20 to 50 μm. The size of the corundum crystals increases with increasing pressure and increasing concentration of cerium. The synthesized α-Al_2O_3 : Ce^{3+} reveals a luminescent band in the UV region at 352 nm and a blue band at 421 nm. The intensity of the cerium ion luminescence in corundum increases with an increase in the water fluid pressure during synthesis. The follow-up annealing of α-Al_2O_3 : Ce^{3+} at 1400°C in a vacuum leads to a decrease in the luminescence. It has been concluded that spectrally active complex structures that include cerium ions, oxygen vacancies, and hydroxyl groups are produced in the media of a supercritical water fluid upon the synthesis of boehmite and corundum. Exposure to high temperatures causes their transformation.

Keywords: corundum, boehmite, cerium doping, optical properties, solid-phase synthesis in a supercritical water fluid.

DOI: 10.3103/S0027131411050087

INTRODUCTION

In connection with the development of new sources of light, e.g., light-emitting diodes (LED), among which white LEDs are in the most demand [1], technologies for manufacturing luminescent materials that emit in the ultraviolet (UV) and blue regions of the optical spectrum [1] are of great importance. To produce a white LED, luminescent material that emits in the ultraviolet and blue region of the spectrum is covered by a powder of yellow luminophor. When the LED is operating, blue radiation of the substrate excites yellow emission of the luminophor powder, and the mixed colors produce white light.

Corundum doped with Ce^{+3} ions is one of the luminophors which radiate blue light [2]. A procedure for the preparation of an yttrium–aluminum garnet doped with cerium ($Y_3Al_5O_{12}$:Ce) in an water fluid, a luminophor with green-yellow emission, has been suggested in [3]. The composition of these two luminophors can be used to craft a white LED.

A method for the preparation of fine crystalline corundum doped with Ce^{3+} ions in an aqueous supercritical fluid (ASCF) is reported in the present work.

High-temperature techniques for the synthesis of doped corundum have been described in [4–6]. Earlier, we developed a method of the synthesis of corundum and some complex oxides doped with such elements as Cr, Mn, Co, and Eu [7–10]. This method has been used in the present studies for the synthesis of α-Al_3O_3:Ce. The aim of the work is to obtain fine crystalline corundum doped with cerium that exhibits high-intensity UV and blue photoluminescence.

EXPERIMENTAL

Aluminum hydroxide, Al_2O_3 of the GD-00 brand (Pikalevo Alumina Factory, assay 99.6%) and cerium nitrate, $Ce(NO_3)_3 \cdot 6H_2O$ (assay 99.99%) were used in the synthesis of fine crystalline corundum. The concentration of cerium ions (Ce^{3+}) in reaction media was calculated in relation to the final product, aluminum oxide.

An aqueous suspension of the reagent mixture was placed in a 12–18 mL autoclave equipped with an insert of stainless steel. The autoclave was heated to 415°C at a rate of about 3°C/min and kept at this temperature for a certain time. The water fluid pressure at 415°C reached up 21.6–31.6 MPa depending on the extent of occupancy of the autoclave free volume.

The phase composition of the synthesized products and the coherent scattering domain size (CSDS) in

the powder were investigated using a STOE-1P and DRONE-3M X-ray diffractometer with Cu $K\alpha$-radiation. The broadening of diffraction reflexes and their shifts can be used both for the determination of the sizes of nanocrystallites in the boehmite and corundum crystals and for the evaluation of the degree of defectiveness of the microcrystals. The latter characteristic can be quantitatively expressed through the value of CSZ [11–15]. Determination of the dimensions of CSZ was performed using graphical analysis of the diffraction line patterns with *hkl* indices which corresponded to (1 2 0) for boehmite and (1 0 2) for corundum.

The photoluminescence spectra were registered on a SDL-2M spectrometer by excitation with 254 nm light (a DRK-120 lamp in the glowing arc mode). To record the luminescence excitation spectra, a DKsSh-150 lamp was used. The dimensions and morphology of the crystals were studied using a *Cam Scan Series 2* and *JSM-639OLA* electron microscope. The size distribution of the corundum crystals was determined by analysis of the SEM microphotographs using the method of linear segments. The diffuse reflectance spectra of the synthesized products were observed in the region from 220 to 900 nm on a *Specord M40* spectrophotometer using $BaSO_4$ as a reference. Spectra of complementary absorption were obtained by subtraction of the diffuse reflectance spectra of samples synthesized at lower and higher concentrations of cerium. Thermogravimetric analyses of the samples were carried out in a dynamic mode in an argon atmosphere (20 mL/min) by using a *Netzsch STA 449C* derivatograph combined with a *Netzsch Aelos QMS 403C* quadrupole mass spectrometer.

RESULTS AND DISCUSSION

Conversion of hydrargillite into corundum in water media that contains cerium ions, as well as in the presence of other ions [7, 8, 13], takes place with the intermediate formation of boehmite (AlOOH). The full conversion of hydrargillite into boehmite in hydrothermal conditions is achieved at temperatures above 200°C. Boehmite transforms into corundum with a further increase in temperature to values that are higher than the critical temperature (374°C). Kinetic curves for the conversion of boehmite into corundum in a supercritical fluid at 415°C and concentrations of cerium ions in reaction media equal to 0.02 and 0.25 wt % are shown in Fig. 1. The starting points of the kinetic curves correspond to a temperature of 415°C and an ASCF pressure of 29.6 MPa. An induction period of 5 hours precedes the formation of corundum crystals, over which only boehmite is detected. As shown in Fig. 1, when the concentration of cerium ions in reaction media increases from 0.02 to 0.25 wt %, the time for the full conversion of boehmite into corundum increases correspondingly from 11 to 13.5 hours. The same figure depicts the linearization of the kinetic curves in coordinates that correspond to the equation

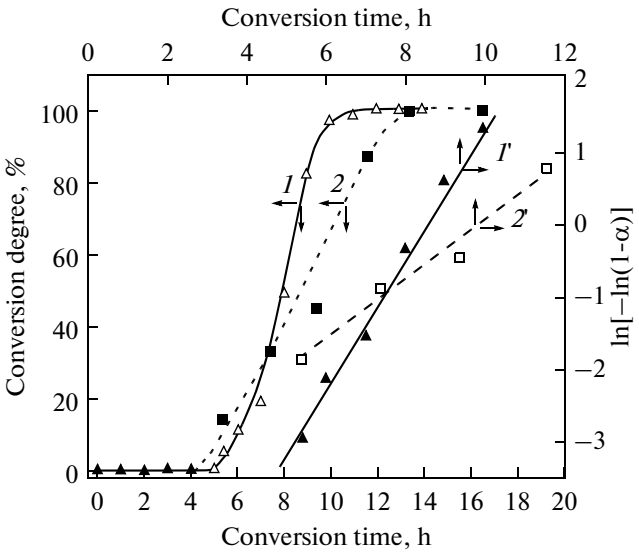

Fig. 1. Kinetic curves of the formation of corundum at 415°C and a SCAF pressure of 29.6 MPa. The contents of cerium ions in the reaction media are 0.02 wt % (*1*) and 0.25 wt % (*2*). Linearization of the kinetic dependences (*1*' and *2*').

$$\ln[-\ln(1-\alpha)] = kt + c, \quad (1)$$

where α is the degree of conversion of boehmite into corundum and k is the rate constant for the nucleation [13], which describes transformation by the solid-phase mechanism. Nucleation and growth of the corundum crystals take place in the solid phase due to an increase in the crystal lattice mobility under conditions of a quasiequilibrium hydroxylation–dehydroxylation process of boehmite in the ASCF atmosphere [7, 13]. The inclination angle of the linearized kinetic dependence (Fig. 1) determines the rate constant for the nucleation of corundum (1) [13]. Powder X-ray diffraction and thermogravimetric analyses (Fig. 2) showed that, within the interval of the induction period which precedes the formation of corundum, the boehmite structure is preserved and the water content is reduced with an increase in the time of exposure of boehmite in ASCF. The derivatograms of boehmite that was doped with cerium and obtained by heating the reaction system until attaining the isothermic level at 415°C are shown in Fig. 3. Figure 3 also shows the flux densities of water and carbon dioxide that are evolved with the heating of the boehmite sample, which are registered using mass-spectrometric techniques. The derivatogram shows a pronounced endothermic effect in the temperature interval from 450 to 600°C, with a maximum at 558°C. The main release of water from the boehmite structure with the formation of weakly structured aluminum oxide takes place in this temperature range. The weight loss due to the liberation of water from the structure of boehmite is con-

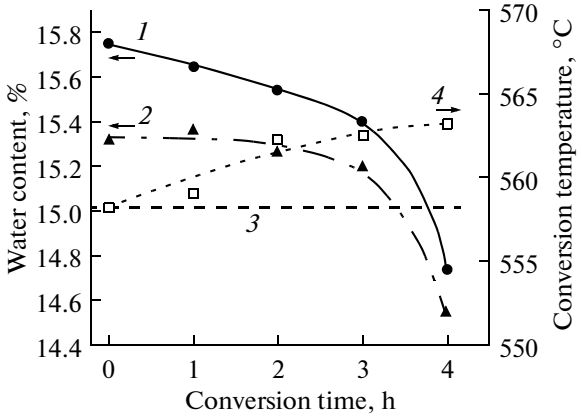

Fig. 2. Changes in the water content of boehmite in the induction period of its transformation to corundum: (*1*) corresponds to the total content, (*2*) to the content of the structural water, and (*3*) to the stoichiometric content of water in boehmite, (*4*) illustrates an increase in the temperature of decomposition of boehmite upon heating during thermogravimetric analysis. Synthesis conditions: $T_{synth} = 415°C$, $P_{H_2O} = 29.6$ MPa, $C(Ce^{3+}) = 0.25$ wt %, and the synthesis time is 0–4 h.

firmed by the mass-spectrometric detection of a beam with a mass number of $m/z = 18$ (H_2O) (Fig. 3). The decrease in the weight of boehmite in the 200–400°C interval with an ill-defined maximum at 343°C is caused by the desorption of water located on the surface of well-dispersed particles in the intercrystallite boundaries [16] and water that is coordinated by aluminum in the $d_{(020)}$-interlayer space [17]. As found in the present work, boehmite treated with an water fluid contains water in amounts substantially higher than the stoichiometric ratio (Fig. 2). After exposure of boehmite for 4 h at 415°C and an water fluid pressure of $P_{H_2O} = 29.6$ MPa, the amount of water yielded in the 200–400°C interval decreased by more than two times, and the total amount of water fell from 15.31 to 14.54%, i.e., to a value less than the stoichiometric content (15.0157%). With further exposure in the ASCF media, reorganization of the boehmite structure into the corundum structure starts. Both the heat effect and the temperature of thermal decomposition during the thermogravimetric analysis of boehmite increase with an increase in the duration of the induction period.

The size of the coherent scattering zone (CSZ) of boehmite increases during the induction period (Fig. 4), which indicates a reduction in the defectiveness of its structure with the time of its treatment in a supercritical water fluid. This is also indicated by the decrease in the parameters of the elementary unit cell of boehmite during the induction period (Table 1). A similar CSZ dependence on the time of the reaction process is also observed for the obtained corundum, since the average size of the coherent scattering zone in corundum increases from 58 to 80 nm after 8 h of hydrothermal

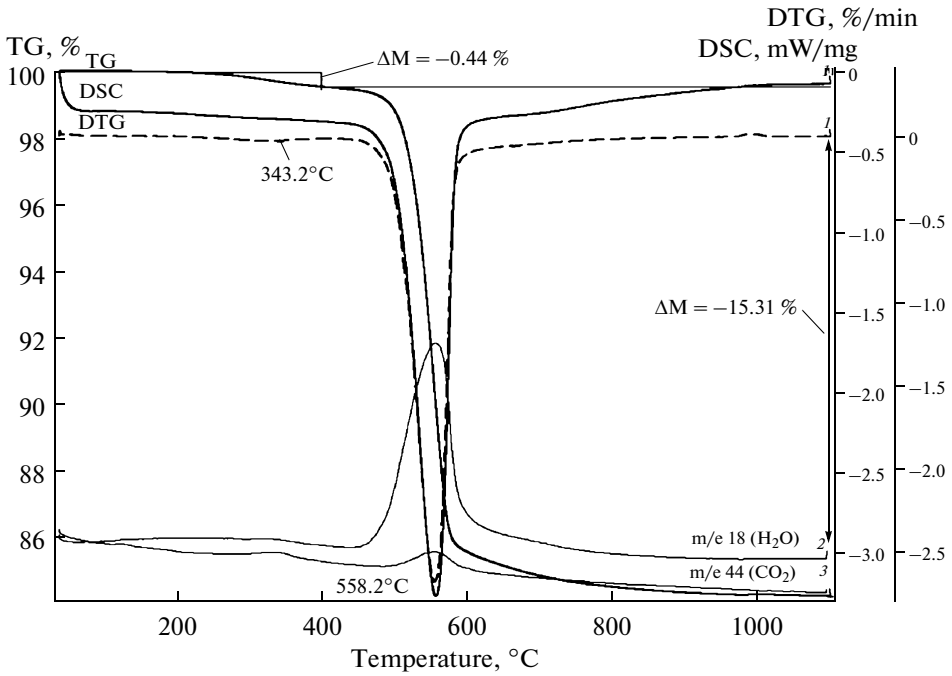

Fig. 3. Derivatogramm of boehmite synthesized at 415°C, $P_{H_2O} = 29.6$ MPa, and $C(Ce^{3+}) = 0.25$ wt % at the start of an induction period ($t = 0$ h).

treatment at micron-level sizes of the formed crystals (Fig. 4).

During the induction period, morphological changes in boehmite take place and nuclei of corundum crystals appear. SEM images of the starting hydrargillite particles, the aggregates of the obtained boehmite, and the emerging crystals of corundum are shown in Fig. 5. The characteristic morphology of the hydrargillite spherullites (Fig. 5, a and b) persists in the initial steps of the formation of boehmite (Fig. 5, c and d). At the end of the induction period, the first corundum crystals appear against the background of numerous micron-level crystals of boehmite (Fig. 5, d, e). The formation of the first corundum crystals goes through oriented cocrystallization of boehmite (Fig. 5, d) with a synchronized structural rearrangement. In the meantime, the corundum crystals grow and their habits change (Fig. 5, d, e). At the end of the transformation of boehmite into corundum, a powder of well-faceted monocrystals of corundum (Fig. 5, f) with sizes from 10 to 100 μm is obtained. The mean size of the crystals increases with an increase in the ASCF pressure and the growth of the ion content in the reaction media (Tables 2 and 3).

The increase in the average dimension of the corundum crystals with an increase in the ASCF pressure (Table 2) indicates a change in the ratio between the nucleation and growth rates of the corundum crystals. The corundum crystals grow to the detriment of the smaller particles of boehmite, which transform and merge with the surface of the larger corundum crystals (Fig. 5).

The inclusion of cerium ions in the synthesized boehmite and corundum is revealed in the diffuse reflectance (DR) spectra of the samples (Fig. 6); specifically, boehmite generates the band at 309 nm (Fig. 6, a, inset) and corundum the band at 330 nm (Fig. 6, b, inset). This fact allows one to conclude that the doping of the aluminooxide substrate takes place at the stage of the formation of boehmite from hydrargillite. Cerium ions that are present in the reaction media take part in the reorganization of the crystal lattice of hydrargillite

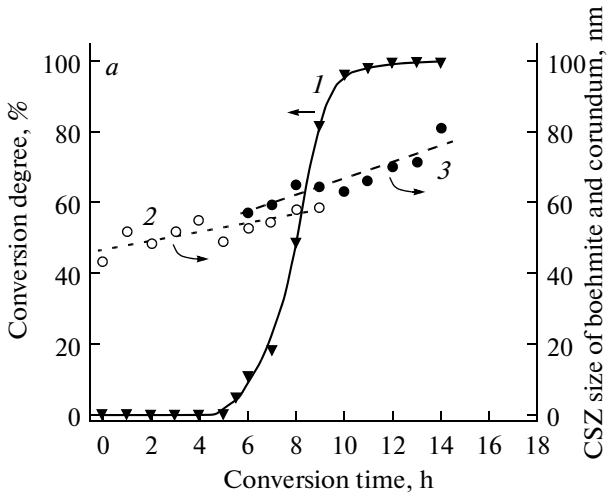

Fig. 4. Kinetic curve of the formation of corundum from boehmite (*1*) and the changes in the CSZ size of boehmite (*2*) and corundum (*3*) at 415°C, SCAF pressure of 29.6 MPa, and 0.02 wt % content of cerium ions in reaction media.

with the formation of boehmite in the process of reversible dehydroxylation. The doped boehmite forms corundum doped with cerium ions. The absorption bands in the DR spectra of the doped boehmite and corundum have complicated patterns, with certain components more distinguishable for the doped corundum. At least three bands of light absorption can be discriminated in the DR spectra of the doped corundum: the two which are associated with Ce^{3+} are revealed near 330 and 549 nm, and the other, which has to be assigned to F^{+}-centers (charged vacancies of the oxygen ions) of the corundum structure, is revealed near 236 nm (Fig. 6, b). Analogous bands have been observed with the doping of corundum with manganese ions [13].

The differential spectrum between the DR spectra for the doped and non-doped corundum (Fig. 6, b, inset) more clearly reveals the additional absorption band at

Table 1. Unit cell parameters of boehmite at different times of synthesis

	Time of synthesis, h				Difference in parameters, Å
	0		4		
	Parameter, Å	Error	Parameter, Å	Error	
a	2.87069	0.00024	2.87025	0.00036	0.00044
b	12.23214	0.0018	12.22756	0.0024	0.00458
c	3.69728	0.00032	3.69660	0.00044	0.00068

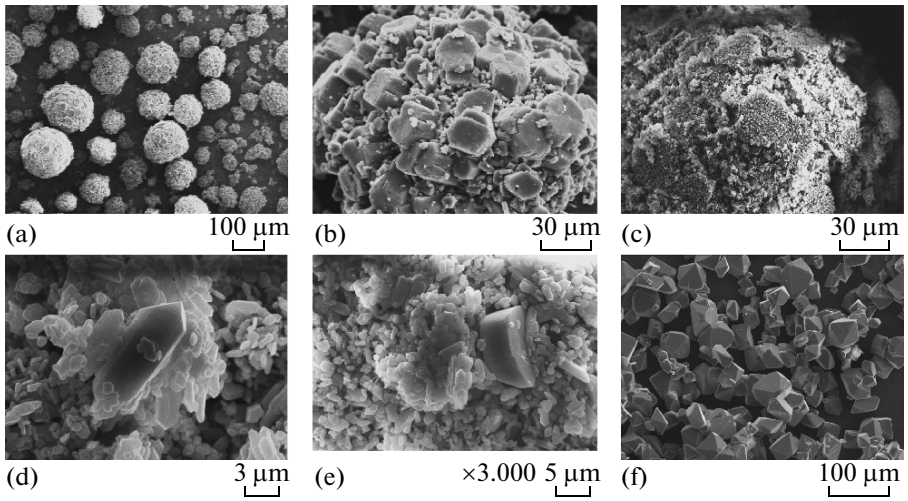

Fig. 5. Microphotographs of particles of hydrargillite (a and b), aggregates of boehmite (c), particles of boehmite with the inclusion of corundum nuclei (d), growing corundum crystals (e), and the final corundum crystals (f). Synthesis conditions: temperature of 415°C, SCAF pressure of 29.6 MPa, and cerium content in reaction media of 0.25 wt %.

330 nm, which is caused by cerium ions in the structure of the doped corundum.

The dependence of a Kubelka–Moon function,

$$F(R) = (1 - R)^2/2R, \quad (2)$$

where R is the diffuse reflectance [18, 19], on the content of cerium ions in the structure of the doped corundum for its absorption band at 330 nm is shown in Fig. 7.

A Kubelka–Moon function with consistent outer conditions (grain size, wavelength, and temperature) is proportional to the molar concentration of the ion that absorbs light in a sample. The linearity of the $F(R)$ function suggests the homogeneous incorporation of cerium ions into the structure of corundum, samples of which have been synthesized for a wide range of cerium ion concentrations in reaction media (Fig. 7).

Table 2. Dependence of the size of the corundum crystal (d) on the SCAF pressure (0.02 wt % content of cerium ions, 415°C, synthesis time of 21 h)

SCAF pressure, MPa	$d \pm 0.1$ μm
21.6	34.9
24.4	35.1
26.4	41.1
29.6	47.7
31.6	54.3

The analogous spectral patterns of corundum and boehmite that are doped with cerium in the case of both emission and excitation luminescence (Figs. 8 and 9) indicate the uniformity of their spectrally active centers. Since both corundum and boehmite doped with cerium have a wide band in the interval from 230 to 450 nm, the luminescence of samples was excited by 254 nm light. Cerium ions undergo a transition to the Ce^{3+}(5d)-excited state upon irradiation by this light. An intense band with the characteristic doublets at 314 and 333 nm is observed in the luminescence spectrum of boehmite (Fig. 8, a), which is usually assigned to a 5d–4f electron transition of the excited Ce^{3+} ions [20, 21]. The intense band with a maximum near 351 nm in the luminescence spectrum of corundum doped with cerium is related to that transition as well (Fig. 8, b). The luminescence band near 420 nm is usually ascribed to the F-centers [22–24]. There are also narrow emission bands from contaminants of Mn^{4+} and Cr^{3+} ions in the red region of the luminescence spectrum of corundum.

The change in the luminescence intensity of boehmite and corundum during their formation in a reaction media containing 0.02% of cerium is shown in Fig. 9. During the induction period, the band intensity of the Ce^{3+} luminescence in boehmite with a maximum at 332 nm decreases. Maximal quenching of luminescence is observed after the treatment of boehmite in a SCAF for 5–6 hrs. Over this time, the dehydroxylation of boehmite takes place. The increase in the luminescence intensity of cerium ions after the end of the induction period is caused by the formation of

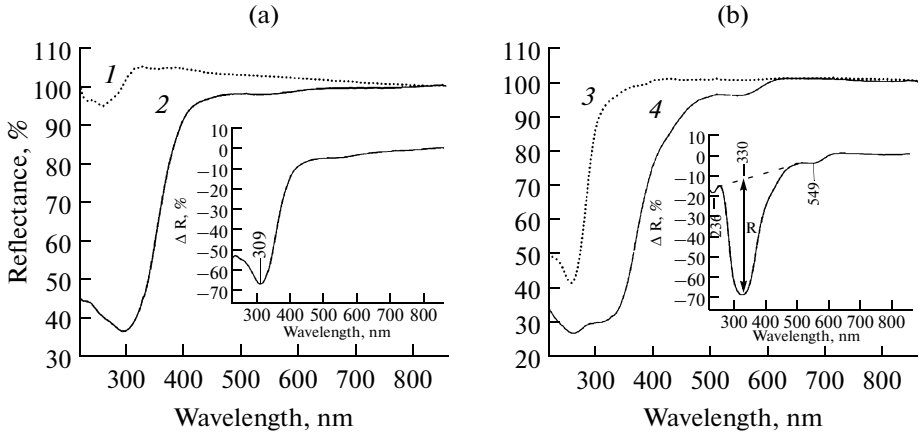

Fig. 6. Diffuse reflectance spectra of boehmite (a) and corundum (b) for both pure and cerium-ion-doped, (a) (*1*) corresponds to the nondoped boehmite (synthesis time of 1 h), (*2*) to the doped boehmite (synthesis time of 1 h); (b) (*3*) corresponds to the nondoped corundum (synthesis time of 23 h), (*4*) to the doped corundum (synthesis time of 16.5 h). The synthesis temperature is 415°C, C(Ce^{3+}) = 0.25 wt %, and P_{H_2O} = 29.6 MPa. The supplementary absorption spectra are given in the insets. The method for determination of the band intensity (*R*) for the Kubelka–Moon function is given in the b inset.

the doped corundum. The luminescence spectrum of the samples after the conversion of boehmite into corundum acquires the typical appearance (Fig. 8, b). The maximum of the luminescence band shifts to the red side of the spectrum (350 nm) in conjunction with the formation of corundum and the changing environment of cerium ions in the aluminooxide matrix (Fig. 9). A redshift of the luminescence band is also observed for samples of corundum obtained at a higher content of cerium in reaction media (Fig. 10). The maximum of the luminescence band shifts from 337 to 373 nm with an increase in the concentration of cerium in reaction media from 0.001 to 0.05 wt % (Fig. 10, Curve *1*). The maximal luminescence intensity corresponds to a cerium concentration in reaction media equal to 0.005 wt % (Fig. 10, Curve *2*). The shift of the maximum of the luminescence band of corundum occurs within the interval of cerium content in reaction media from 0.001 to 0.05 wt % (Fig. 10). The redshift of the luminescence band at 320 nm in the DR spectrum of corundum (Fig. 12, absorption spectra, *a*, *b*, and *c*, and the differential spectra in the inset) also corresponds to this area. An increase in the concentration of cerium in reaction media and, consequently, in the structure of corundum also gives rise to an increase in the intensity of the luminescence band at 320 nm and its broadening. The synthesis of corundum and the incorporation of cerium ions in its structure in the media of a supercritical fluid are accompanied by the formation of charged anion vacancies (*F*-centers, band near 238 nm). Judging by the DR spectral patterns, the multiplicity of the states of a cerium ion in corundum is expanded by the emergence of the absorption bands near 290, 361, and 403 nm (inset in Fig. 11), when the content of cerium ions is increased within the 0.05–0.09 wt % interval, as well as near 549 nm at the 0.25% content of cerium ions (Fig. 6, b, inset).

The uniformity of the excitation spectra of Ce^{3+} ions in boehmite and corundum (inset in Fig. 8, a and b) and the presence of the luminescence peak at 421 nm in both cases allow one to presume that photons of the excitation light are absorbed by the charged oxygen vacancies (in a form of the *F*-centers), and the excitation energy is transferred to Ce^{3+} ions with the subsequent luminescence. It has been demonstrated earlier [25] that doping with rare earth ions during the synthesis of oxides in a SCAF leads to a high content of vacancies in the oxygen sublattice. The specifics of the synthesis of corundum in a SCAF allow one to presume that the anion vacancies can also react with the remaining hydroxyl groups. The luminescence intensity of the synthesized samples of corundum, which depends on the SCAF pressure at the 21.6–31.6 MPa

Table 3. Dependence of the size of the corundum crystal (*d*) on the content of Ce ions in reaction media. The conditions of synthesis are as follows: P_{H_2O} = 29.6 MPa, T = 415°C, synthesis time of 21 h)

Content of Ce^{3+} ions in reaction media, %	Mean size of crystals, $d \pm 0.1$ μm
0.01	31.7
0.05	32.2
0.07	33.4
0.09	36.3
0.25	49.2

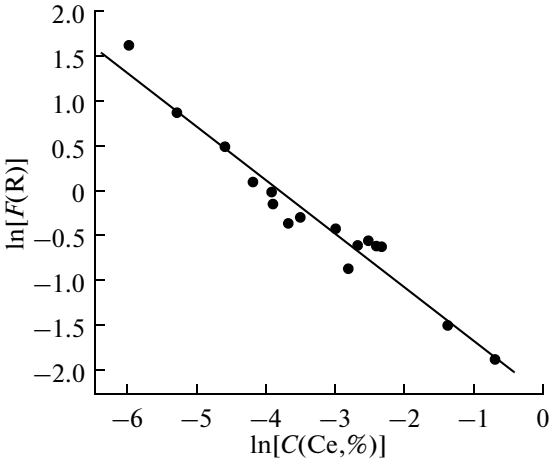

Fig. 7. Dependence of the Kubelka–Moon function for the absorbance band of cerium ions in corundum at 330 nm on the cerium content in reaction media. Conditions of corundum synthesis: synthesis temperature of 415°C and SCAF pressure of 29.6 MPa.

interval, is presented in Table 4. Increases in the SCAF pressure and, as a consequence, in the content of hydroxyls in corundum lead to an increase in the luminescence intensity. Thus, the luminescent properties of both boehmite and corundum depend on the presence of hydroxyl groups in the structure. The annealing of corundum doped with cerium in a vacuum at 1800°C for 1 h leads to the removal of hydroxyl groups from the structure of corundum and causes the quenching of the luminescent bands of cerium ions (Fig. 9, Spectra *1* and *2*). The dehydroxylation of corundum synthesized in a SCAF with annealing is accompanied by the formation of oxygen vacancies and the growth in the intensity of the 436 nm band of the *F*-centers (Fig. 12, Spectra *2* and *3*). It should be noted that annealing in air for 1 h at 1400°C leads to the full quenching of the luminescence band of the Ce^{3+} ions (Fig. 12, Spectrum *3*); this could be caused by the destruction of the luminescence centers and the oxidation of cerium ions to the Ce^{4+} state. In this case, an increase in the luminescence intensity of the *F*-centers (λ is the same observed).

The negative effect of the high-temperature heating on the luminescence intensity, as well as the influence of cerium ions on the rate of formation of corundum, allow one to conclude that cerium ions react with hydroxyl groups in the aluminooxygen matrix and form with them a complex that also includes the *F*-centers. With high-temperature heating, the removal of the remaining hydroxyl groups from the structure of the doped corundum takes place, and the spectroscopic active center is destroyed with the formation of the *F*-centers and the cerium ions with a changed charge. The authors of [26–28] have also determined the effect of anion vacancies on the luminescent properties of ion actuators in solid luminophors.

It should be noted that the spectrum of the optical emission of the synthesized α-Al_2O_3:Ce^{3+} (Fig. 8, b), which comprises the two broad bands near 350 and 420 nm, corresponds to the excitation spectrum of garnet, $Y_3Al_5O_{12}$:Ce^{3+}, which exhibits luminescence in the yellow interval (450–650 nm) with a maximum at 528 nm and is synthesized in similar conditions [3]. Hence, the emission of Al_2O_3:Ce^{3+} can be used for the excitation of the green-yellow luminescence of $Y_3Al_5O_{12}$:Ce^{3+}. In addition, the combination of the blue and yellow radiation creates a color gamma that is close to white light.

Upon the treatment of hydrargillite in a SCAF in the presence of cerium ions, the synthesis of corundum proceeds with the intermediary formation of doped boehmite. The doping of boehmite with cerium

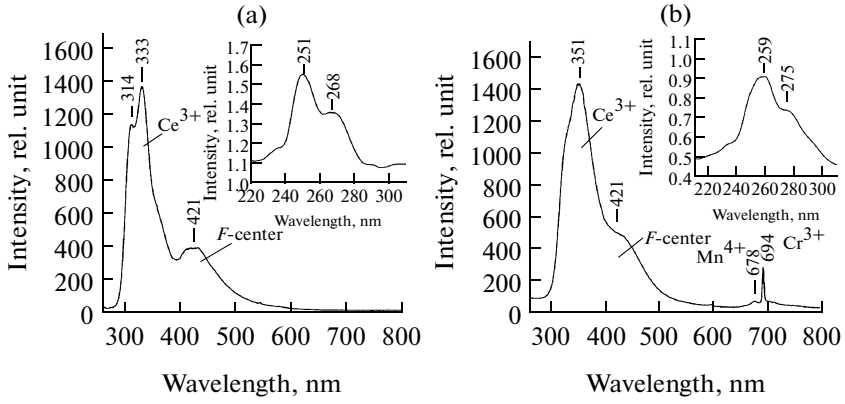

Fig. 8. Luminescence spectra of boehmite (a) and corundum (b) synthesized at 415°C in a SCAF containing 0.02% of cerium ions. The synthesis time of boehmite is 2 h and the SCAF pressure is 29.6 MPa. The synthesis time of corundum is 35 h and the SCAF pressure is 21.6 MPa. The excitation spectra of the luminescence bands at 333 nm (a) and 351nm (b) are given in the inset.

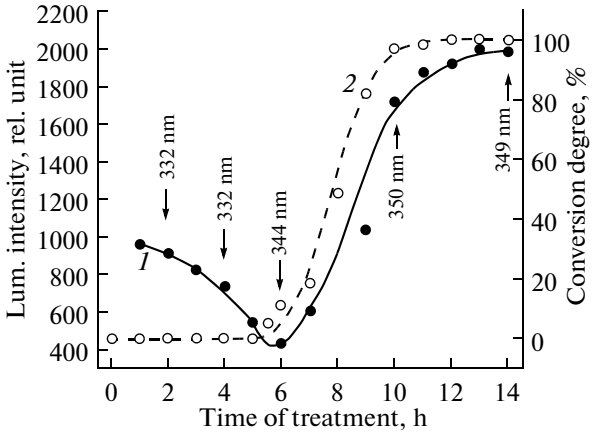

Fig. 9. Dependence of the luminescence band intensity of the Ce^{3+} ions (*1*) and the composition of the formed corundum (*2*) on the reaction time. $C(Ce^{3+}) = 0.02$ wt %, $P_{H_2O} = 29.6$ MPa, and $T_{synth} = 415$°C. The arrows indicate the band maxima in the luminescence spectra.

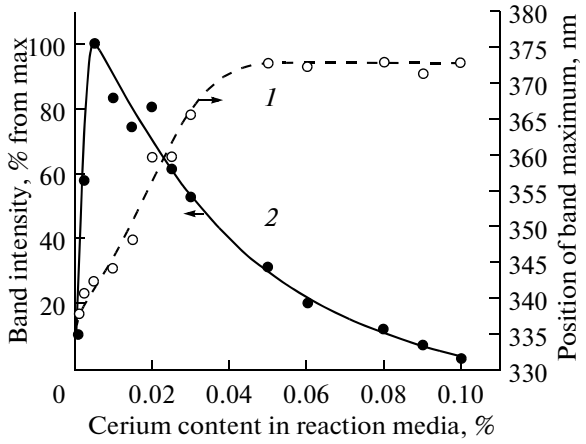

Fig. 10. Dependence of the wavelength (*1*) and the intensity (*2*) of a luminescence maximum of the doped corundum on the cerium content in reaction media. Conditions of synthesis: $P_{H_2O} = 29.6$ MPa, $T_{synth} = 415$°C, and time of synthesis 20–25 h.

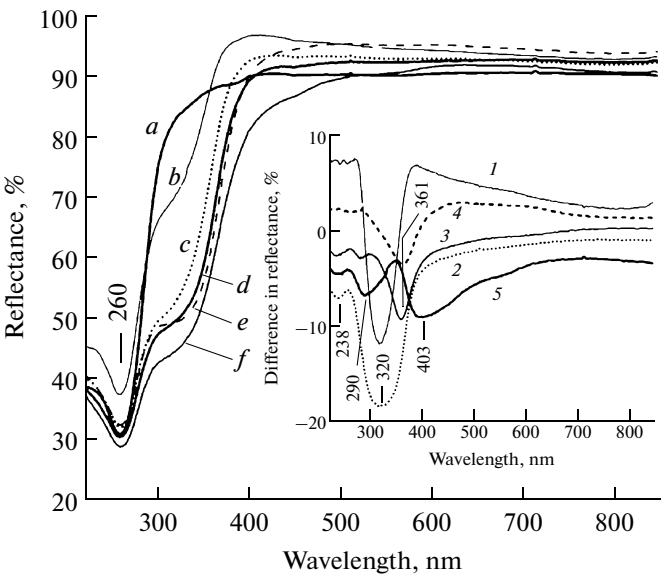

Fig. 11. Diffuse reflectance spectra of corundum with the different contents of cerium (wt % in reaction media): *a* for 0.001, *b* for 0.01, *c* for 0.03, *d* for 0.05, *e* for 0.07, and *f* for 0.09. The supplementary absorbance spectra are given in the inset: *1* for *b* – *a*, *2* for *c* – *b*, *3* for *d* – *c*, *4* for *e* – *d*, and *5* for *f* – *e*.

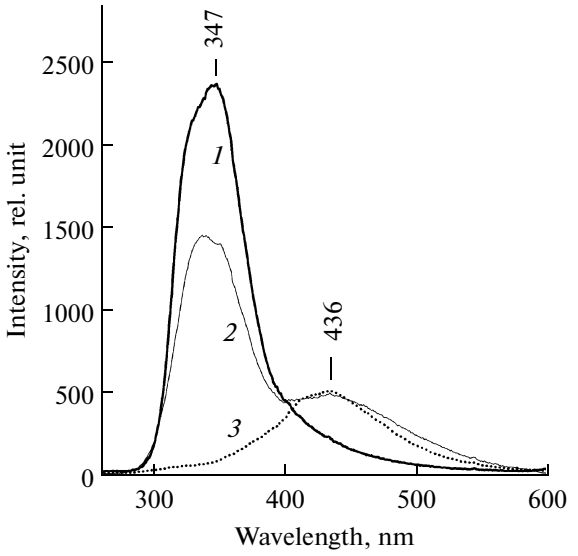

Fig. 12. Effect of annealing doped corundum on its luminescence intensity, where *1* corresponds to the luminescence spectrum of corundum doped with 0.02 wt % of cerium before annealing, *2* to the spectrum after 1 h of annealing in a vacuum at 1800°C, and *3* to the spectrum after 1 h of annealing in air at 1400°C.

takes place in the stage of the transformation of hydrargillite into boehmite with the incorporation of cerium ions from the reaction media to its structure, due to the mobility of the crystal lattice in the conditions of a hydroxylation–dehydroxylation quasiequilibrium process. Upon the formation of corundum from boehmite doped by this method, the Ce^{3+} ions are homogeneously distributed in the volume of the formed corundum crystals. The Ce^{3+} ions incorporated in the structure of both corundum and boehmite exhibit intense luminescence in the UV and blue region. The maximal intensity of the luminescence of cerium ions is observed in corundum synthesized at the 0.005 wt % content of cerium in reaction media. An increase in the SCAF pressure during the synthesis increases the luminescence intensity. It has been concluded that an emission center on the basis of cerium ions includes oxygen vacancies in a form of *F*-centers and hydroxyl groups which stabilize the cerium ion state in the form of Ce^{3+} ions. The synthesized corun-

Table 4. Dependence of the luminescence intensity of corundum on the SCAF pressure for the band at 351 nm (T_{synth} = 415°C, synthesis time of 20–25 h, C(Ce^{3+}) = 0.02 wt %)

SCAF pressure, MPa	Intensity of the 351 nm luminescence band of corundum
21.6	253
24.4	782
26.4	803
29.6	890
31.6	1541

dum can be used together with the yttrium–aluminum garnet, which is a luminophor with green-yellow emission, in the manufacture of white LEDs.

ACKNOWLEDGMENTS

The authors are grateful to M.V. Lobanov for help in determination of the unit cell parameters of boehmite.

REFERENCES

1. Dimple P. Dutta and Tyagi, A.K., *Solid State Phenom.*, 2009, vol. 155, p. 113.
2. Ba, D., Liao, G., We, L., Liu, S., and Yan, S., *J. Vac. Sci. Technol.*, 2006, vol. 26, no. 5, p. 421.
3. Danchevskaya, M.N., Ivakin, Yu.D., Maryashkin, A.V., and Murav'eva, G.P., *Sverkhkrit. Fluidy Teor. Prakt.*, 2010, vol. 5, no. 4, p. 90.
4. Aono, K., Toida, H., Terashima, K., and Iwaki M., *Nucl. Instrum. Methods*, 2001, vol. B175–177, p. 580.
5. Merzhanov, A.G., Borovinskaya, I.P., Prokudina, V.K., Pesotskaya, N.S., and Nasonova, M.A., *Nauka Proizvodstvu*, 1998, vol. 8, no. 10, p. 4.
6. Mygkov, V.G., Polyakova, K.P., Bondarenko, G.N., and Polyakov, V.V., *Fiz. Tverd. Tela*, 2003, vol. 45, no. 1, p. 131.
7. Danchevskaya, M.N., Ivakin, Yu.D., Torbin, S.N., Muravieva, G.P., and Ovchinnikova, O.G., *ISHA Newsletter*, 2008, vol. 3, p. 12.
8. Danchevskaya, M.N., Ivakin, Yu.D., Muravieva, G.P., and Luchkov, I.V., *J. Phys.: Conf. Ser.*, 2008, vol. 121. doi 10.1088/1742-6596/121/8/082001.
9. Danchevskaya, M.N., Ivakin, Yu.D., Bagdasarov, Kh.S., Antonov, E.V., Kostomarov, D.V., and Panasyuk, G.P., *Perspekt. Mater.,* 2009, vol. 4, p. 28.
10. Ivakin, Yu.D., Zui, Murav'eva, G.P., and Danchevskaya, M.N., *Vestn. Mosk. Univ., Ser. 2: Khim.*, 2001, vol. 42, no. 4, p. 258.
11. Streletskiy, A.N., Lapshin, V.I., and Fokina, E.L., *Kinet. Kataliz*, 1989, vol. 30, p. 1064.
12. Danchevskaya, M.N., Torbin, S.N., Muravieva, G.P., Ovchinnikova, O.G., Ivakin, Yu.D., *React. Solid.*, 1988, vol. 5, p. 293.
13. Ivakin, Yu.D., Danchevskaya, M.N., Ovchinnikova, Muravieva, G.P., and Kreisberg, V.A., *Sverkhkrit. Fluidy Teor. Prakt.*, 2008, vol. 3, no. 4, p. 11.
14. Sharenkova, N.V., Kaminskiy, V.V., Romanova, M.V., Vasil'ev, L.N., and Kamenskaya, G.A., *Fiz. Tverd. Tela,* 2008, vol. 50, no. 7, p. 1158.
15. Shtol'z, A.K., Medvedev, A.I., and Kurbatova, L.V., *Rentgenovskiy analiz mikronapryazhenii i razmera oblastei kogerentnogo rasseyaniya v polikristallicheskikh materialakh* (X-ray Diffraction Analysis of Microstrains and Sizes of Coherent Scattering Zones in Polycrystalline Materials), Ekaterinburg, 2005.
16. Shefer, K.I., Analysis of Defects in the Structures of Hydroxides and Oxides of Aluminum on the Basis of X-ray Diffraction Data, *Cand. Sci. (Chem.) Dissertation*, Novosibirsk, 2008.
17. Okada, K., Nagashima, T., Kameshima, Y., Yasumori, A., and Tsukada, T., *J. Colloid Interf. Sci.*, 2002, vol. 253, p. 308.
18. Kortyum, G., Braun, V., and Gerzog, G., *Usp. Phiz. Nauk*, 1965, vol. 85, no.2, p. 365.
19. Kubelka, P., *Spektroskopiya otrazheniya (Tepriya, metody, praktika)* (Reflectance Spectroscopy: Theory, Techniques, and Practice), Moscow, 1978.
20. Stryganyuk, G., Trots, D.M., Voloshinovskii, A., Shalapska, T., Zakordonskiy, V., Vistovskyy, V., Pidzyrailo, M., and Zimmerer, G., *J. Lumin.*, 2008, vol. 128, p. 355.
21. Ternane, R., Cohen-Adad, M.Th., Panczer, G., Goutaudier, C., Dujardin, C., Boulon, G., Kbir-Ariguib, N., and Trabelsi-Ayedi, M., *Solid State Sci.*, 2002, vol. 4, p. 53.
22. Lee, K.H. and Crawford, J.J.H., *Phys. Rev.*, 1977, vol. B15, p. 4065.
23. Evans, B.D. and Stapelbroek, M., *Phys. Rev.,* 1978, vol. B18, p. 7089.
24. Lee, K.H. and Crawford, J.J.H., *Phys. Rev.*, 1979, vol. B19, p. 3217.
25. Kazakov, V.P. and Lapshin, A.I., *Zh. Teor. Eksperim. Khim.*, 1971, vol. 7, no. 1, p. 133.
26. Kompan, M.E., Boikov, Yu.M., Melekh, B.A., and Yakubovich, A.V., *Phiz. Tverd. Tela,* 2002, vol. 44, no. 7, p. 1211.
27. Clabau, F., Rocquefelte, X., Le Mercier, T., Deniard, P., Jobic, S., and Whangbo, M.-H., *Chem. Mater.*, 2006, vol. 18, no. 14, p. 3212.
28. Zhdanov, E.A., *Zh. Prikl. Spektrosk.,* 1985, vol. 42, no. 4, p. 639.